Characterization of low-enthalpy geothermal resources and evaluation of potential contaminants

Franco Frau, Rosa Cidu, Giorgio Ghiglieri & Guglielmo Angelo Caddeo

Rendiconti Lincei. Scienze Fisiche e Naturali

ISSN 2037-4631

Rend. Fis. Acc. Lincei
DOI 10.1007/s12210-020-00950-6

Springer

Your article is protected by copyright and all rights are held exclusively by Accademia Nazionale dei Lincei. This e-offprint is for personal use only and shall not be self-archived in electronic repositories. If you wish to self-archive your article, please use the accepted manuscript version for posting on your own website. You may further deposit the accepted manuscript version in any repository, provided it is only made publicly available 12 months after official publication or later and provided acknowledgement is given to the original source of publication and a link is inserted to the published article on Springer's website. The link must be accompanied by the following text: "The final publication is available at link.springer.com".

Author's personal copy

Rendiconti Lincei. Scienze Fisiche e Naturali
https://doi.org/10.1007/s12210-020-00950-6

Characterization of low-enthalpy geothermal resources and evaluation of potential contaminants

Franco Frau[1] · Rosa Cidu[1] · Giorgio Ghiglieri[1] · Guglielmo Angelo Caddeo[1]

Received: 25 May 2020 / Accepted: 6 August 2020
© Accademia Nazionale dei Lincei 2020

Abstract
The use of renewable resources alternative to fossil fuels, thus contributing to the reduction of CO_2 emissions, requires the assessment of eventual negative impacts on the environment. This study was devoted to the characterization of low-enthalpy geothermal resources and the potential contamination of geothermal effluents into the aquatic system. Thirty-five groundwater samples were collected in the Campidano (southern Sardinia, Italy), an area showing heat flow anomalies and thermal occurrences. Hydrogeological features inferred by literature were implemented by data acquired at each sampling site. Physical–chemical parameters, major, minor and trace components in groundwater were determined, together with the isotopic composition of the water. Six hydrogeological units with variable permeability were identified. According to geological and hydrogeological modeling, four of the six units appeared hydraulically connected, although not everywhere. The predominant groundwater flow was seen from north-east to south-west. The water temperature was in the range 17–42 °C, pH ranged from 6.7 to 8.6, dissolved oxygen varied from < 0.2 to 7.8 mg L^{-1} and electrical conductivity from 0.8 to 10 mS cm^{-1}. Predominant cations were Na^+ and Ca^{2+}, predominant anions were either Cl^- or HCO_3^-. The more saline waters showed anyhow a marked Na^+–Cl^- chemical composition. Most waters were found either at near equilibrium with respect to calcite or slightly saturated, but under saturated with respect to gypsum. Isotopic values of δ^2H and $\delta^{18}O$ in the water samples indicated a meteoric origin. Particular attention was paid to potential contaminants, which should be evaluated when thermal waters are used in spa treatments and balneology. Concentrations of NO_3^- and NH_4^+ above the Italian limits established for drinking water (50 mg L^{-1} and 0.5 mg L^{-1}, respectively) occurred in one oxygenated groundwater and five reduced groundwater samples, respectively. Fluoride concentrations exceeding the Italian limit of 1.5 mg L^{-1} were observed in three groundwater samples. The mean value of As was 3.2 µg L^{-1}, with one groundwater exceeding the 10 µg L^{-1} of the legal value. The groundwater with the highest temperature (42 °C), an artesian well, was characterized by relatively high concentrations of Cl^-, F^-, Li, B, Ge, Rb, Mo, Cs, W, Sc and Ga. Overall results allowed to identify the area most suitable for geothermal exploitation. Deep fluids, probably located at a depth > 1 km, would rise up along faults or fractured zones in the granitic–metamorphic Paleozoic basement. Maximum temperatures of 90 °C in the thermal reservoir were estimated by silica and Na–K–Ca geothermometers. The $\delta^{18}O$ enrichment shift occurring at high temperature was not observed. Due to high concentrations of some contaminants (e.g. Mo, W, B, F^-), geothermal effluents derived from exploitation should be either re-injected or treated before discharge for avoiding the contamination of aquatic systems.

Keywords Thermal water · Hydrogeology · Geochemistry · Trace elements · Contaminants · Sardinian resources

1 Introduction

Due to the increasing demand for renewable and clean energy resources, the geothermal energy is attracting relevant attention worldwide because it can provide energy 24-h-a-day (Li et al. 2018), and can allow significant reduction of CO_2 emissions, as compared to the use of fossil fuel power plants (Yousefi et al. 2019). An estimation of worldwide applications of geothermal energy for

Electronic supplementary material The online version of this article (https://doi.org/10.1007/s12210-020-00950-6) contains supplementary material, which is available to authorized users.

✉ Rosa Cidu
cidur@unica.it

[1] Department of Chemical and Geological Sciences, University of Cagliari, Blocco A, Monserrato, Italy

Published online: 18 August 2020

Author's personal copy

direct utilization at the end of 2014 was 70,885 MWt, corresponding to a 46.2% increase over the 2010 data (Lund and Boyd 2016). Direct use of geothermal energy—such as heating/cooling of buildings, balneology, aquaculture, heat supply for greenhouse and factories—can be sometimes limited due to legal, economic and social issues. Limiting factors may include: lack of adequate legislation, development risk and cost, inability in technology transfer and social acceptance (Minissale 2018; Yasukawa et al. 2018; Noorollahi et al. 2019). Developments of geothermal energy may have either positive or negative environmental consequences in specific areas (Manzella et al. 2018). Among negative effects, geothermal effluents released into the environment may pose human health at risk, frequently due to high concentrations of toxic and/or harmful components, such as As, B, Hg and F^- (Shortall et al. 2015). Therefore, geothermal energy projects should be developed together with a sustainability assessment plan, for which several tools and frameworks currently exist (Strategic Environmental Assessment EU Directive 2001/42/EC; Shortall et al. 2015). Geochemical studies of thermal waters provide an effective tool for investigating potential impact on the environment due to geothermal exploitation, thus providing useful information to improve social acceptance (Yasukawa et al. 2018). Therefore, this research was focused on the characterization of groundwater chemical parameters for assessing environmental impacts in areas with potential exploitation of geothermal energy.

The study area is located in the southern Campidano, Sardinia, Italy. In this area, anomalous values of heat flow have been recognized (Loddo et al. 1982; D'Amore et al. 1987; Cataldi et al. 1995; Angelone et al. 2005), suggesting favorable conditions for the development of geothermal energy. In fact, the Sardinian Region has recently received several requests for a permit of geothermal exploration in the southern Campidano. The study area is close to the metropolitan city of Cagliari hosting some 500,000 inhabitants, which represent a good pool of potential uses of geothermal energy. In the study area, detailed studies on groundwater resources were not undertaken so far, characterization being limited to one artesian well with water temperature of 40 °C. Specific objectives of this study were: (i) the assessment of local hydrogeological conditions, (ii) the hydrogeochemical characterization of groundwater samples located nearby the thermal well, (iii) the characterization of isotopic composition of waters, (iv) the occurrence of trace elements including toxic/harmful species and (v) the evaluation of temperature in the deep aquifer. Information derived from this study will result useful for considering the use of geothermal resources in south Sardinia.

2 Study area

2.1 Geology

Superimposed extensional and trans-tensional events in the Miocene resulted in the formation of the Sardinian Rift, which extends from the Gulf of Cagliari to the Gulf of Asinara (Faccenna et al. 2002). The southern part of the Sardinian Rift is defined Campidano Graben (Cherchi and Montadert 1982; Carmignani et al. 2001), hereafter Campidano. It extends from the Gulf of Cagliari to the Gulf of Oristano, as shown in Fig. 1, and shows boundary faults with maximum throws up to 3000–4000 m (Balia et al. 1984). The N–S trending faults bounding the northern Campidano and the offshore Sardinian basin could be directly related to the opening of south Tyrrhenian basin; the NW–SE trending master faults in the southern Campidano are related to the reactivation of structures developed from late Paleozoic to the Oligo-Miocene (Cocco et al. 2012, 2013).

The Campidano basement is made up of predominant Paleozoic granitic–metamorphic rocks, whereas the depression is filled by sedimentary and volcanic formations of Tertiary and Quaternary age (Pala et al. 1982; Balia et al. 1984; Egger et al. 1988; Casula et al. 2001). The Campidano underwent a subsiding cycle in the Middle Pliocene, with the southern part being filled by sand, mud, conglomerate, lacustrine clay and fluvial deposits (Angelone et al. 2005 and references therein).

2.2 Thermal manifestations

Climate is Mediterranean with warm dry summers and mild rainy winters. The mean annual temperature is 15.9 °C and annual precipitation is 537 mm, the latter mostly concentrated between October and March.

Detailed geothermal investigations in the Campidano were carried out in the 1980s, in the framework of projects funded by the European Community and the Italian National Research Council (e.g. Bertorino et al. 1982a, b; Pala et al. 1982; Caboi et al. 1983; Balia et al. 1984, 1991; D'Amore et al. 1987). In the Campidano Graben, the main thermal manifestations occur at Santa Maria Is Acquas Sardara (60 °C, Balia et al. 1985), S'Acquacotta Villasor (46 °C, Bertorino et al. 1982a), Su Campu Monastir (43 °C, Frau 1994) and Sa Guardia Uta (34 °C, Bertorino et al. 1982a), which locations can be seen in Fig. 1. Results of geophysical investigations indicated that the thermal occurrences correspond to local manifestations, related to the rise up, from the granitic–metamorphic complex, of deep fluids along fault segments or fractured zones (Angelone et al. 2005).

Author's personal copy

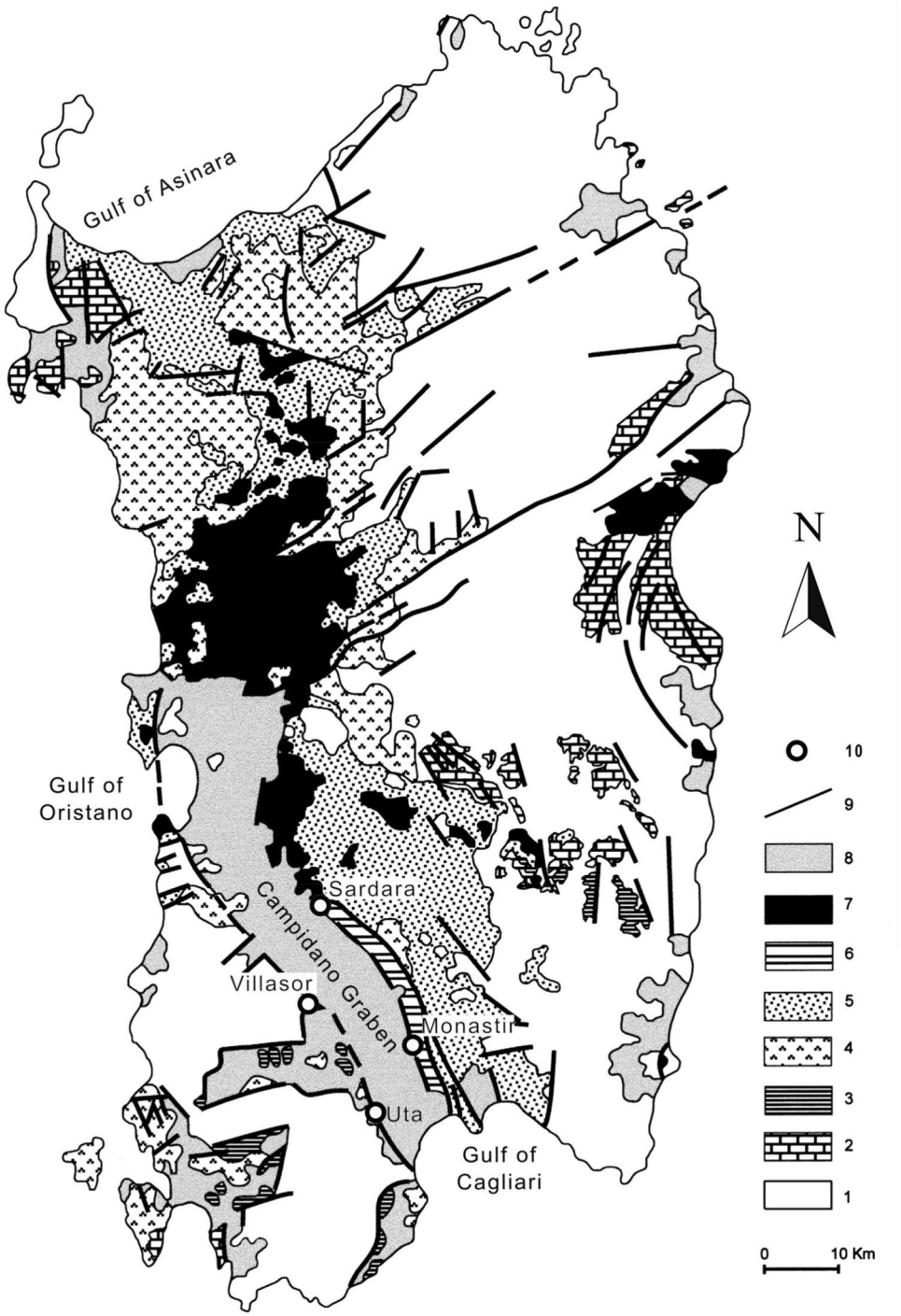

Fig. 1 Geological features of Sardinia (modified after Casula et al. 2001) showing the Campidano Graben and main thermal water occurrences. Legend: (1) Paleozoic basement; (2) Permian-Mesozoic rocks; (3) Paleocene-Eocene sediments; (4) Oligo-Miocene volcanic rocks; (5) Oligocene to Neogene deposits; (6) Pliocene continental deposits; (7) Pliocene–Quaternary volcanic rocks; (8) Quaternary sediments; (9) faults; (10) thermal waters

Heat flow anomalies were recognized in the Campidano Graben (Loddo et al. 1982; D'Amore et al. 1987; Cataldi et al. 1995). A mean value of 188.4 mW/m^2 was observed at Sardara and the thermal gradient was estimated at 1 °C per 15–20 m (Angelone et al. 2005). The calculated quartz equilibrium temperature at undefined source depth was 120 °C in the Central Campidano (Bertorino et al. 1982b). In the regional gravity map, the western part of the Campidano Graben shows a regular trend of positive anomalies and fault systems on both sides throughout its length: the iso-contour lines are elongated parallel to the main axis and form a positive gravity trend from the centre towards SW (Guerra 1981; Egger et al. 1988). The Bouguer map is dominated by a negative anomaly, extending approximately NW–SE from Oristano to Decimomannu (nearby Uta in Fig. 1), that was correlated with magnetometric data, and may be related to the Tertiary filling of the Campidano, made up of Miocene–Pliocene sediments

Author's personal copy

(Balia et al. 1984, 1991). Gravity highs correspond predominantly to outcrops of the Paleozoic crystalline basement and to the Tertiary andesitic rocks. A remarkable correspondence between high gravimetric–magnetometric gradients and thermal springs was observed (Balia et al. 1984). Favorable conditions for geothermal exploitation likely occur in the southern Campidano: a relevant fault system and a thermal gradient of 68 °C/km was recognized nearby Uta (Loddo et al. 1982); high geophysical horizontal gradients, ^{222}Rn values up to 251 Bq/L and recent seismicity were observed in the Capoterra sector, south of Uta in Fig. 1 (Angelone et al. 2005).

3 Sampling and analytical methods

For this study, an area located in the southern Campidano was identified taking into account literature results on heat flux (Loddo et al. 1982; Caboi et al. 1983; Balia et al. 1984; Angelone et al. 2005) and the occurrence of thermal water (Frau 1993, 1994). A total of 35 groundwater samples were collected during a survey carried out in June 2011. Their location is shown in Fig. 2. The depth of wells ranged from 70 to 220 m below ground level (b.g.l., Table 1). Those wells not in use under the survey were purged 20 min before sampling.

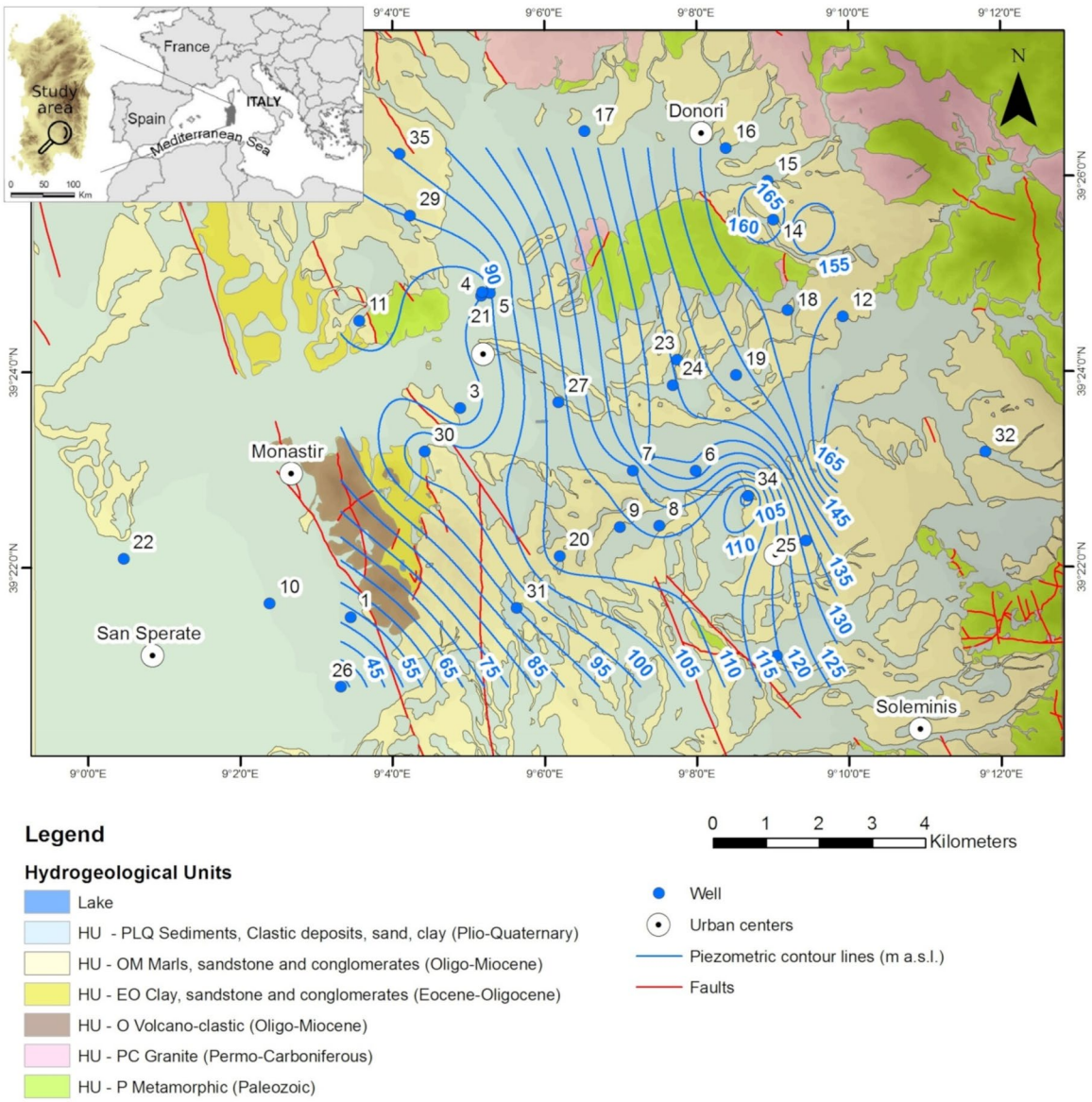

Fig. 2 Schematic geological map of the study area (modified after www.sardegnageoportale.it; Casula et al. 2001) showing locations of the groundwater sampling sites and the piezometric contour lines

Author's personal copy

Table 1 Coordinates, well depth and level of water in the Campidano samples

Sample	UTM Coordinates		Depth	Water table
No	Nord	East	m b.g.l	m b.g.l
1	39° 21′ 31.9″	9° 03′ 26.0″	116	6.0
2	39° 23′ 11.1''	9° 07′ 21.4''	100	2.3
3	39° 23′ 40.07″	9° 04′ 52.3″	220	13.0
4	39° 24′ 49.1''	9° 05′ 09.0''	86	0.3
5	39° 24′ 50.6″	9° 05′ 15.8″	83	4.3
6	39° 23′ 01.3''	9° 07′ 58.2″	130	13.4
7	39° 23′ 01.6″	9° 07′ 08.7″	100	21.6
8	39° 22′ 27.7''	9° 07′ 29.6″	197	29.2
9	39° 22′ 26.9″	9° 06′ 58.4″	180	50.2
10	39° 21′ 40.4″	9° 02′ 21.9″	200	0.0
11	39° 24′ 33.7''	9° 03′ 32.8″	100	0.8
12	39° 24′ 36.1″	9° 09′ 54.4″	100	nd
13	39° 25′ 31.8″	9° 09′ 21.0″	70	19.3
14	39° 25′ 35.6″	9° 08′ 59.7″	85	10.5
15	39° 25′ 59.4″	9° 08′ 55.2″	100	3.2
16	39° 26′ 19.5″	9° 08′ 22.3″	115	8.8
17	39° 26′ 29.9″	9° 06′ 30.7″	100	nd
18	39° 24′ 39.9″	9° 09′ 11.0″	100	28.6
19	39° 24′ 00.1″	9° 08′ 30.0″	80	0.0
20	39° 22′ 09.1″	9° 06′ 10.8″	205	57
21	39° 24′ 51.1″	9° 05′ 09.8″	90	0.5
22	39° 22′ 07.7″	9° 00′ 26.8″	100	nd
23	39° 24′ 09.6″	9° 07′ 43.6″	100	nd
24	39° 23′ 54.1″	9° 07′ 40.4''	nd	nd
25	39° 22′ 18.3″	9° 09′ 25.2″	190	nd
26	39° 20′ 49.2″	9° 03′ 18.1″	130	24.5
27	39° 23′ 43.6″	9° 06′ 10.0″	200	17.6
28	39° 21′ 08.0″	9° 09′ 00.2″	152	17.4
29	39° 25′ 38.3″	9° 04′ 13.0″	100	nd
30	39° 23′ 13.4″	9° 04′ 24.3″	160	3.0
31	39° 21′ 37.9″	9° 05′ 36.4″	200	nd
32	39° 23′ 12.9″	9° 11′ 46.7″	140	nd
33	39° 23′ 03.9″	9° 09′ 49.6''	180	20
34	39° 22′ 46.1″	9° 08′ 39.4″	160	20
35	39° 26′ 16.0″	9° 04′ 04.8″	120	nd

m b.g.l. meters below ground level, *nd* not determined

The hydrogeological features of the study area were inferred by the official 1:25,000 map of Sardinia, available in digital form at www.sardegnageoportale.it. The stratigraphic data of wells were elaborated from literature (CASMEZ 1976; Pala et al. 1982; Casula et al. 2001) and from unpublished works carried out by the Authors. At each well, technical data, elevation and geographical coordinates using a Garmin global positioning system, and piezometric levels using an Electric Contact Meter Type KLL Seba GmbH Instrument, were acquired. The data were inserted into a digital database and GIS, using the ArcGIS v10.0 program.

Groundwater flows were reconstructed on the basis of the piezometric data acquired during the survey (Table 1) creating a contour line map as shown in Fig. 2. According to the hydrogeological model, the piezometric data were attributed to the hydrogeological unit of the Plio-Quaternary sediments. The hydraulic head values were computed by subtracting the observed water levels from elevations, then mapped using geostatistical interpolation techniques (Kriging process).

At sampling sites, temperature, pH, redox potential (Eh), electrical conductivity (EC), dissolved oxygen (DO) and alkalinity were measured. The Eh was measured with a platinum electrode and values were corrected against the ZoBell's solution (Nordstrom 1977). Alkalinity was measured both in the field and in the laboratory by titration with HCl (using methyl orange as indicator) and the Gran function plot method, respectively. The CO_3^{2-} ion was < 1 mg L^{-1}, thus was not reported. For both chemical and isotopic determinations, the water was filtered through 0.22 µm pore-size filters immediately upon collection and stored in pre-cleaned high-density PE bottles. Samples were cooled in situ using a portable refrigerator. A filtered aliquot was used for the determination of major cations, anions and the nitrogen species (NO_3^-, NO_2^-, NH_4^+) by ionic chromatography (IC, Dionex ICS3000). Two filtered aliquots were acidified (supra pure HNO_3 1% v/v) on site for major and trace analyses by inductively coupled plasma optical emission spectrometry (ICP-OES, ARL3520) and ICP mass spectrometry (ICP-MS, PerkinElmer SCIEX ELAN DRC-e), respectively. One filtered aliquot was acidified (supra pure HCl 0.5% v/v) on site for the determination of As by hydride generation ICP-MS (Cidu 1996).

The detection limits (DL) were calculated at 10 times the standard deviation (SD) value calculated on several analyses of the blank solution (ultrapure water MILLI-Q with supra pure HNO_3 1%, v/v). Field blank solutions were prepared daily and analyzed for assessing eventual contamination during sampling. The standard reference solutions SRM1643e (supplied by the US National Institute of Standard & Technology, Gaithersburg, Maryland), EnviroMAT ES-L-2 and EP-H-3 (supplied by SCP Science, St. Laurent, Quebec) were used to estimate analytical errors, which were $< 5\%$ at mg L^{-1}, $< 10\%$ at µg L^{-1} and $< 20\%$ at ng L^{-1} levels. The ionic balance calculated by the code DIAGRAMMES (Simler 2012) was below 4%, except one sample showing 7%. Major and trace elements were determined at the Department of Chemical and Geological Sciences, University of Cagliari, Italy. Concentrations of potential contaminants were evaluated with respect to limits established in drinking water, a precautionary principle for the reduction of hazards

Author's personal copy

to the human health (WHO 2011), especially when thermal waters are used in spa treatments and balneology.

The isotopic values of δ^2H and $\delta^{18}O$ of waters were determined by isotope ratio mass spectrometry at the Italian Research Council (CNR) facilities in Pisa (Italy). Results were expressed in terms of delta notation per mil (Coplen 2011) relative to the Vienna Standard Mean Oceanic Water (V-SMOW). Analytical errors calculated using international and internal laboratory standards were ± 1 ‰ for δ^2H and ± 0.2 ‰ for $\delta^{18}O$.

The computer program PHREEQC (Parkhurst and Appelo 1999) was used to calculate the saturation index (SI) values.

4 Results and discussion

4.1 Hydrogeology

Results of hydraulic head surveys carried out in this study, and the parameters permeability, saturated thickness and specific yield inferred from the stratigraphic well logs and unpublished technical reports, allowed to transform the geological information into hydrogeological parameters. Six hydrogeological units (HU) were identified and described, from the top to the bottom, as follows.

1. HU-PLQ. This unit is represented by a multi-layer aquifer hosted in the Plio-Quaternary sedimentary sequence (clastic deposits, sand, clay). Alluvial sediments occupy the river valleys and often lie above ancient alluvial terraces. Thickness is greater at the centre of the Campidano Graben reaching several hundred meters. Alluvium deposits are made up of fan fluvial and alluvial sediments, in turns composed of conglomerates, gravels and sands, with different degree of compaction, sometimes interbedded with silt-clayey levels. This variability, extending both laterally and at depth, resulted in different permeability values, from 10^{-3} to 10^{-7} m s^{-1}.
2. HU-OM. This unit is represented by a multi-layer aquifer, sometimes confined, hosted in the Oligo-Miocene marl, sandstone and conglomerate. The average thickness is 200 m. The average permeability was 10^{-7} m s^{-1}, but increased (10^{-4} m s^{-1}) where low-cemented conglomerate levels occur.
3. HU-EO. This unit is represented by a multi-layer aquifer, sometimes confined and hosted in the Eocene–Oligocene sandstone and conglomerate. The average thickness is 200 m and average permeability is 10^{-4} m s^{-1}.
4. HU-OQ. This unit is hosted in a volcano-clastic sequence. Several volcanic events affected the evolution of the Sardinia Cenozoic Graben system (including the Campidano), starting from the Oligo-Miocene with calc-alkaline volcanism (gabbro- tonalitic- bodies, ignimbrites interbedded with andesite) to Plio-Quaternary with alkaline volcanic events (mainly basalt lava flows). The permeability occurs in the fractured part of this unit allowing a good groundwater circulation.
5. HU-PC. This unit hosts a granite fractured aquifer. Granitic rocks are indeed extensively fractured and show secondary permeability at the transition to piedmont deposits, laminated on the top areas and significantly altered even at depth. The presence of faults can promote deep groundwater circulation or act as impermeable barrier.
6. HU-P. This unit is hosted in a metamorphic complex, namely meta-sandstones and quartzite interbedded whit phyllites and mica schist, and shows low permeability (10^{-7} m s^{-1}).

Figure 2 shows the hydrogeological sketch map. According to the geological and hydrogeological interpretation we can assert that the units HU-PLQ, HU-OM and HU-EO are here hydraulically connected, although not everywhere. Groundwater flows were reconstructed on the basis of the piezometric data acquired during the field survey. The piezometric contour lines indicate a predominant groundwater flow direction from the NE to the SW sector of Fig. 2.

4.2 Hydrogeochemical features

Analytical results are reported in Tables 2 and 3, and in the Supplementary material S1. During the survey the air temperature was in the range of 20–32 °C with a mean of 25 °C. The water temperature was in the range of 17–42 °C (Table 2) and showed poor correlation ($R^2 = 0.24$) with the well depth. Values of pH ranged from 6.7 to 8.6, Eh from 0.03 to 0.46 V, DO from < 0.2 to 7.8 mg L^{-1} and EC from 0.8 to 10 mS cm^{-1} (Table 2). The EC values ≤ 1 mS cm^{-1} mainly occurred in the NE sector of the study area (i.e. samples Nos. 12 to 18), whereas high EC values were observed in the SW (i.e. samples Nos. 10, 26, 30, 31; Fig. 2). The water N. 10 Su Campu showed physical–chemical characteristics and concentrations of dissolved components similar to those observed in 1990 (Frau 1994), indicating that it is a water with deep circulation poorly affected by seasonal variations. The Piper diagram in Fig. 3 shows the relative proportions of major ions. Predominant cations were Na^+ and Ca^{2+}, whereas Mg^{2+} was generally subordinate. Predominant anions were either Cl^- or HCO_3^-, but sample No. 31 showed a predominant SO_4^{2-} composition. Water samples with high values of EC showed a marked Na^+–Cl^- chemical composition. Concentrations of Cl^- in groundwater located in the SW sector were above the estimated background range for groundwater interacting with Tertiary and Quaternary sediments of the Campidano (Biddau et al. 2017). Positive correlation ($R^2 = 0.91$) between Na^+ and Cl^- was observed

Author's personal copy

Table 2 Water temperature (T), electric conductivity (EC), pH, redox potential (Eh), dissolved oxygen (DO) concentrations of major components and isotopic composition of the Campidano waters

Sample	T	EC	pH	Eh	DO	Ca	Mg	Na	K	HCO_3^-	Cl^-	SO_4^{2-}	NO_3^-	NH_4^+	F^-	Br^-	SiO_2	$\delta^{18}O/‰$		$\delta^2H/‰$		*d*
No.	°C	mS cm^{-1}		*V*	Mg L^{-1}													Mean	SD	Mean	SD	
1	21	2.65	7.2	0.28	4.6	130	85	413	19	600	375	450	0.7	0.31	0.28	1.4	33.0	− 4.91	0.10	− 32.0	0.43	7.2
2	21	1.3	7.2	0.30	2.2	96	32	162	5.6	439	163	131	17	< 0.1	0.26	0.6	13.4	− 6.17	0.17	− 36.3	0.82	13.1
3	26	1.72	8.2	0.35	7.0	16	2.4	358	4.4	195	430	74	1.8	< 0.1	4.15	1.6	16.5	− 6.64	0.05	− 40.6	1.17	12.6
4	19	2.48	7.7	0.39	2.2	42	12.4	474	7.6	397	422	320	5.8	0.38	0.52	1.6	11.5	− 5.95	0.09	− 37.5	1.41	10.1
5	17	3.31	7.6	0.20	4.0	88	33	589	10	303	903	157	< 0.1	1.5	0.39	3.2	11.6	− 6.37	0.16	− 39.7	1.30	11.2
6	20	2.8	8.0	0.40	3.0	23	18	629	9.3	503	496	383	6.0	0.37	0.77	1.5	10.8	− 5.70	0.12	− 35.7	1.40	9.9
7	19	1.9	8.0	0.41	4.4	13	6	430	5.6	470	275	231	1.6	0.99	0.99	0.9	9.6	− 5.56	0.19	− 34.3	1.26	10.2
8	21	1.73	7.7	0.14	2.0	39	19	336	5.2	336	334	177	< 0.1	0.79	0.13	0.7	10.7	− 5.90	0.17	− 37.8	0.70	9.4
9	22	1.72	7.9	0.24	6.0	45	19	303	5	342	360	125	< 0.1	0.45	0.23	1.5	19.6	− 6.44	0.12	− 40.4	0.82	11.1
10	42	7.9	8.6	0.10	2.4	560	0.3	1120	12	20	2500	288	< 0.1	0.64	3.04	9.9	31.7	− 5.76	0.18	− 35.2	1.01	10.9
11	21	3.66	7.3	0.20	2.8	89	59	656	14	485	868	280	< 0.1	0.52	2.49	3.1	12.9	− 5.99	0.12	− 36.5	1.10	11.4
12	20	0.82	7.6	0.43	6.0	50	25	72	3.1	232	112	41	3.0	< 0.1	0.04	0.4	20.1	− 6.11	0.11	− 36.6	1.21	12.3
13	21	0.89	7.3	0.44	7.0	61	29	82	3.6	250	156	36	5.5	< 0.1	0.14	0.6	25.3	− 5.58	0.10	− 34.7	0.71	9.9
14	21	0.95	7.5	0.45	7.6	66	29	88	3.9	296	132	42	24	< 0.1	0.02	0.5	28.3	− 6.55	0.14	− 36.5	1.04	15.9
15	16	0.63	6.8	0.46	7.8	49	17	54	1.8	201	76	48	7.5	< 0.1	0.10	0.3	11.5	− 6.87	0.18	− 36.3	0.94	18.6
16	19	0.97	7.5	0.44	6.3	81	31	85	3.7	290	163	76	5.8	< 0.1	0.18	0.6	16.3	− 6.34	0.12	− 37.0	1.11	13.8
17	19	1.04	7.5	0.27	2.2	54	29	119	6.6	308	174	60	0.4	< 0.1	0.32	0.7	18.2	− 6.64	0.19	− 38.1	1.03	15.0
18	20	1.01	7.6	0.43	6.0	56	33	97	4.6	348	157	55	< 0.1	< 0.1	0.03	0.6	16.4	− 6.27	0.12	− 40.5	1.32	9.7
19	20	0.78	7.6	0.15	2.2	36	21	101	2.6	276	122	30	< 0.1	0.14	0.10	0.4	18.4	− 6.02	0.11	− 38.4	1.12	9.8
20	23	1.91	7.5	0.41	1.8	45	24	296	8.1	363	300	168	15	0.38	0.25	1.1	16.7	− 6.54	0.26	− 36.3	0.59	16.0
21	19	2.4	7.5	0.10	< 0.2	59	20	453	7.4	429	340	403	0.2	0.51	0.38	1.5	10.4	− 5.49	0.10	− 33.9	1.28	10.0
22	17	1.57	7.0	0.47	7.0	145	47	141	4.0	430	185	250	55	0.20	0.30	0.7	10.5	− 5.41	0.17	− 32.7	1.28	10.6
23	22	0.75	7.8	0.21	3.0	30	16	132	2.5	323	100	35	< 0.1	0.13	0.28	0.3	18.3	− 7.13	0.20	− 38.3	1.27	18.7
24	22	0.9	8.4	0.19	4.6	7	3.8	189	2.8	345	112	36	< 0.1	2.1	0.17	0.4	14.6	− 6.47	0.15	− 38.1	0.90	13.7
25	21	1.47	7.7	0.46	7.0	84	40	173	11	400	180	206	0.7	< 0.1	0.12	0.6	17.3	− 6.59	0.12	− 37.1	0.56	15.7
26	22	9.78	6.7	0.19	1.2	406	287	1640	48	840	2800	1330	< 0.1	9.2	0.50	9.2	34.5	− 5.35	0.15	− 34.0	1.35	8.8
27	24	2.43	7.3	0.32	2.4	65	31	473	10	476	465	247	1.1	< 0.1	0.29	1.9	15.9	− 6.08	0.13	− 35.1	1.43	13.6
28	19	2.34	7.7	0.25	1.0	53	33	445	6.7	302	525	236	< 0.1	0.43	0.22	1.7	12.1	− 7.03	0.19	− 38.5	0.68	17.7
29	25	1.76	7.6	0.26	4.0	53	24	326	7.0	390	352	151	< 0.1	0.22	0.54	1.2	16.0	− 5.73	0.04	− 35.6	1.35	10.2
30	22	10.5	7.5	0.03	< 0.2	103	46	2310	27	438	3600	444	< 0.1	< 0.1	1.22	14	9.5	− 5.98	0.14	− 34.9	0.85	13.0
31	23	6.3	6.8	0.35	3.0	391	221	1000	28	642	770	2450	4.0	< 0.1	0.42	3.4	13.5	− 5.21	0.19	− 32.9	1.08	8.7
32	20	1.02	7.3	0.45	3.2	66	40	99	4.5	439	112	66	< 0.1	< 0.1	0.11	0.5	22.1	− 6.42	0.10	− 39.2	0.85	12.1
33	20	1.79	7.1	0.41	4.4	168	33	141	6.2	378	285	160	29	< 0.1	0.07	1.2	20.6	− 4.97	0.14	− 35.2	1.41	4.5
34	22	0.82	7.8	0.26	5.0	39	23	119	2.8	358	78	51	< 0.1	< 0.1	0.11	0.4	19.9	− 5.81	0.16	− 36.3	0.90	10.1

Author's personal copy

Table 2 (continued)

Sample No.	T °C	EC mS cm^{-1}	pH	Eh *V*	DO Mg L^{-1}	Ca	Mg	Na	K	HCO_3^-	Cl^-	SO_4^{2-}	NO_3^-	NH_4^+	F^-	Br^-	SiO_2	$\delta^{18}O$/‰		δ^2H/‰		*d*
																		Mean	SD	Mean	SD	
35	19	1.84	7.3	0.28	3.4	138	51	207	8.1	421	280	291	0.3	<0.1	0.15	1.3	13.1	− 5.60	0.08	− 35.3	1.35	9.5

SD standard deviation, *d* (*deuterium excess*) $\delta^2H-8\delta^{18}O$ (Dansgaard 1964)

(Fig. 4a). Many samples showed Na enrichment with respect to seawater, indicating Na^+ contributions from the dissolution of Na-silicate minerals. The No. 10 groundwater was an exception, being Na^+ depleted with respect to seawater (Fig. 4a). This behavior may suggest cation exchange between Na^+ and Ca^{2+}, which is consistent with the relative Ca^{2+} abundance in the No. 10 groundwater (Table 2). Positive correlation ($R^2 = 0.99$) between Br^- and Cl^- was observed and waters were generally aligned along the dilution line of seawater (Fig. 4b).

The waters were either at equilibrium or slightly saturated with respect to calcite, but the No. 5 water was unsaturated (Fig. 5a). The No. 10 groundwater was characterized by a very low value of pCO_2, whereas the No. 26 and No. 31 samples showed the highest pCO_2 values (Fig. 5a). Most of waters were unsaturated with respect to gypsum, except the No. 26 and No. 31 waters that were close to equilibrium (Fig. 5b).

Assuming a precautionary principle for the reduction of hazards to the human health (WHO 2011), concentrations of potential contaminants were compared with limits established in drinking water. Concentrations of NO_2^- and PO_4^{-3} were below 0.1 mg L^{-1} (not reported). Dissolved NO_3^- and NH_4^+ reflected the redox conditions in the water system. Relatively high concentrations of NO_3^- (up to 55 mg L^{-1}) occurred in oxygenated waters characterized by NH_4^+ below 1 mg L^{-1}. The highest value of NH_4^+ (9.2 mg L^{-1}) was observed in the No. 26 groundwater, which is consistent with the low values of DO and Eh observed in this sample (Table 2). Fluoride was in the range from 0.1 to 4.1 mg L^{-1}. Values exceeding the Italian limit of 1.5 mg L^{-1} F^- (G.U.R.I. 2006) were observed in the No. 3, No. 10 and No. 11 groundwater samples (Table 2).

4.3 Isotopic composition of waters

The isotopic composition of the Campidano waters is reported in Table 2. Values of $\delta^{18}O$ ranged from − 7.1 to − 4.9 ‰, δ^2H from − 41 to − 32 ‰ and deuterium in excess (Dansgaard 1964) from 4.5 to 18.7 (Table 2). Figure 6a shows the plot of δ^2H versus $\delta^{18}O$ values in the waters, together with the isotopic composition of local seawater (Cidu et al. 2001). The δ^2H and $\delta^{18}O$ values of the Campidano waters lay between the global meteoric water line (GMWL; Craig 1961) and the Italian meteoric water line (IMWL) proposed for the southern Italy (Giustini et al. 2016). Isotopic values in the Campidano waters were within the range of meteoric waters observed in the north and south Sardinia (Caboi et al. 1993; Cidu et al. 2008) and in Sicily (Giustini et al. 2016). Figure 6b shows chloride concentrations versus $\delta^{18}O$ values in the waters, together with the mixing line between freshwater and local seawater (Cidu et al. 2001). The chloride-rich waters (i.e. samples 10, 26 and 30)

Author's personal copy

Table 3 Concentrations of trace components in the Campidano waters

Sample No.	Li (μg L^{-1})	B (μg L^{-1})	Ge (μg L^{-1})	As (μg L^{-1})	Rb (μg L^{-1})	Sr (μg L^{-1})	Mo (μg L^{-1})	Cs (μg L^{-1})	Ba (μg L^{-1})	W (μg L^{-1})
1	76	358	0.15	1.5	21	2990	25	0.07	21	< 0.5
2	24	236	< 0.05	< 0.4	2.1	1710	1.3	0.03	167	< 0.5
3	91	207	0.45	30.7	3.0	1110	20	0.12	64	6.2
4	185	442	0.29	1.8	5.4	5120	11	0.30	21	< 0.5
5	151	285	0.28	2.5	7.5	10,400	2.7	0.39	42	< 0.5
6	69	721	< 0.1	< 0.4	3.1	1140	3.5	0.05	51	< 0.5
7	107	1160	0.27	< 0.4	2.6	1600	5.2	0.04	15	< 0.5
8	36	230	< 0.05	0.8	2.2	1400	0.8	0.07	25	< 0.5
9	60	360	< 0.1	3.0	4.2	3010	1.2	0.12	50	< 0.5
10	226	3100	4.23	< 0.4	13	2840	59	0.61	73	6.7
11	130	287	0.47	2.9	15	3420	1.2	0.66	31	< 0.5
12	7.4	41	< 0.05	0.9	0.5	378	< 0.5	< 0.02	8	< 0.5
13	9.4	37	< 0.05	2.6	0.4	337	< 0.5	< 0.02	5.4	< 0.5
14	8.6	55	< 0.05	7.3	0.6	300	< 0.5	< 0.02	8.4	< 0.5
15	3.1	25	< 0.05	< 0.4	0.2	84	< 0.5	< 0.02	23	< 0.5
16	10	42	< 0.05	1.2	1.1	398	1.1	0.03	9.5	< 0.5
17	17	75	< 0.05	1.3	3.1	530	2.3	0.06	57	< 0.5
18	12	58	< 0.05	5.8	2.1	412	2.3	0.03	9.7	< 0.5
19	14	69	< 0.05	4.8	2.5	955	0.8	0.04	63	< 0.5
20	75	177	0.05	0.6	4.8	3860	1.2	0.10	51	< 0.5
21	150	270	0.09	2.4	5.6	8900	17	0.19	21	< 0.5
22	6.8	196	< 0.05	< 0.4	0.5	1050	0.9	< 0.02	92	< 0.5
23	14	92	< 0.05	2.6	2.3	475	1.1	0.03	80	< 0.5
24	38	82	< 0.05	< 0.4	2.1	501	1.7	0.06	37	< 1
25	43	168	0.12	2.2	3.1	2380	2.2	0.05	48	< 0.5
26	465	3390	< 0.2	< 0.4	52	11,900	3.2	0.29	69	< 1
27	77	1040	< 0.1	< 0.4	4.3	3270	2.3	0.05	67	< 0.5
28	85	216	0.17	3.1	5.4	3250	4.0	0.11	25	< 0.5
29	53	240	0.19	5.8	5.5	2030	3.4	0.17	35	< 0.5
30	990	1230	0.62	6.6	26	15,100	15	0.73	44	< 1
31	166	834	0.14	< 0.4	6.8	19,800	1.6	0.07	13	< 1
32	24	68	0.06	0.6	2.7	1440	1.1	0.04	71	< 0.5
33	19	97	< 0.05	2.1	1.1	1260	1.0	< 0.02	133	< 0.5
34	21	93	< 0.05	9.4	2.9	1110	1.5	0.06	62	< 0.5
35	51	140	< 0.05	4.2	4.6	1690	13	0.09	44	< 0.5

Author's personal copy

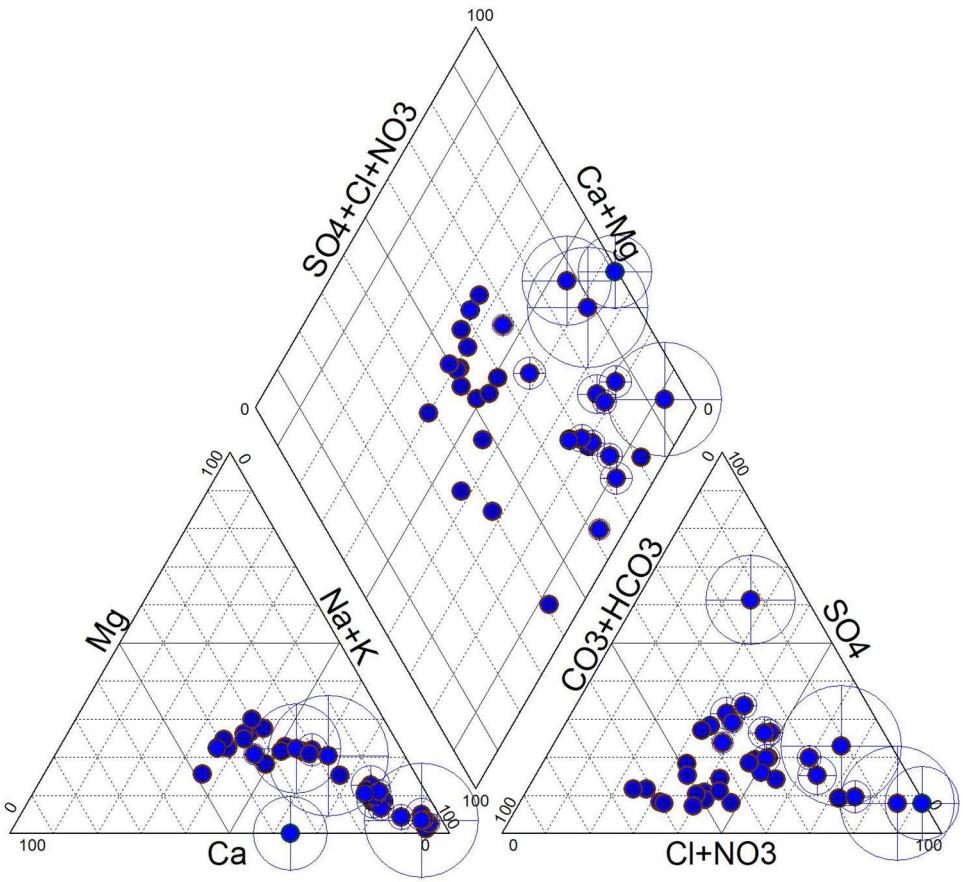

Fig. 3 Piper diagram showing the relative proportions of major ions in the Campidano waters. The size of circles represents the total dissolved solids (TDS), the larger size corresponding to 7.4 g L^{-1}

do not appear significantly affected by mixing processes with modern seawater.

4.4 Trace elements

Concentrations of Be, Sc, Ti, V, Cr, Co, Ga, Se, Ag, Cd, Sb, Te, Tl, Bi and Th were found either below or slightly above detection limits (Supplementary material S1). Elements Al, Ni, Cu, Zn and Pb usually occurred at very low concentrations (Supplementary material S1), i.e. all samples showed values of these elements much below limits established for drinking water (G.U.R.I. 2006; WHO 2011).

Manganese and Fe showed variable concentrations, up to 120 and 3000 µg L^{-1}, respectively. The highest values of Mn and Fe were observed in the No. 21 and No. 26 groundwater samples (Supplementary material S1), which were characterized by low values of Eh and DO, and relatively high concentrations of HCO_3^- and NH_4^+ (Table 2), thus suggesting a reductive dissolution of Mn- and Fe-bearing minerals, a process occurring in reducing environments rich in organic matter (Frau et al. 2019). Arsenic occurred in the range of < 0.4–30.7 µg L^{-1} (Table 3), with mean 3.2 µg L^{-1} and median 1.8 µg L^{-1}, and the No. 3 groundwater exceeding the 10 µg L^{-1} value established for drinking water (G.U.R.I. 2006; WHO 2011).

Concentrations of U, Y and the rare earth elements (REE) were found in a wide range (Supplementary material S1). Values above 2 µg L^{-1} U were observed in oxygenated groundwater; the highest concentration of 16 µg L^{-1} U occurred in the No. 22 groundwater and was associated with the highest concentration of Y + REE (0.27 µg L^{-1}; Supplementary material S1).

The No. 10 groundwater with the highest temperature was characterized by relatively high concentrations of Li, B, Ge, Rb, Mo, Cs and W (Table 3), Sc (5.9 µg L^{-1}, Supplementary material S1) and Ga (0.26 µg L^{-1}, Supplementary material S1). Indeed, the No. 10 groundwater belongs to the outlier samples in the B, Rb, Mo, W, Ge and Cs box-plots shown in Fig. 7. Among other outliers, the No. 30 and No. 26 were distinguished in the Li, B, Rb and Sr box-plots; the No. 3 and No. 30 were distinguished in the As, Mo, and Ge box-plots, as shown in Fig. 7.

Concentrations of B, Li, Rb and Sr, as well as Cl^-, were positively correlated with EC values ($R^2 = 0.680$, 0.760, 0.667, 0.590 and 0.927, respectively). This behavior may suggest either increasing concentrations as the time of interaction of water with rocks increases or increasing

Author's personal copy

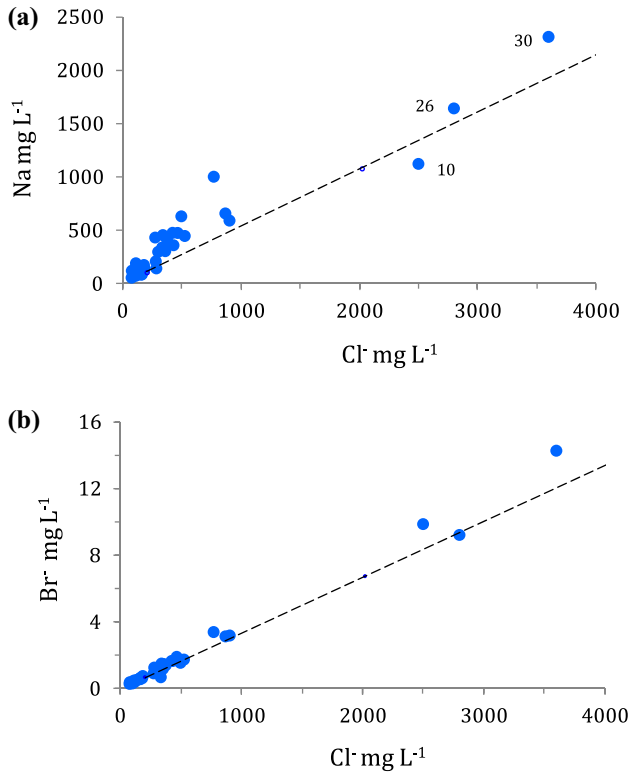

Fig. 4 Plots showing correlations between Na and Cl^- (**a**) and Br^- and Cl^- (**b**) in the studied waters. Dashed lines show the seawater dilution line

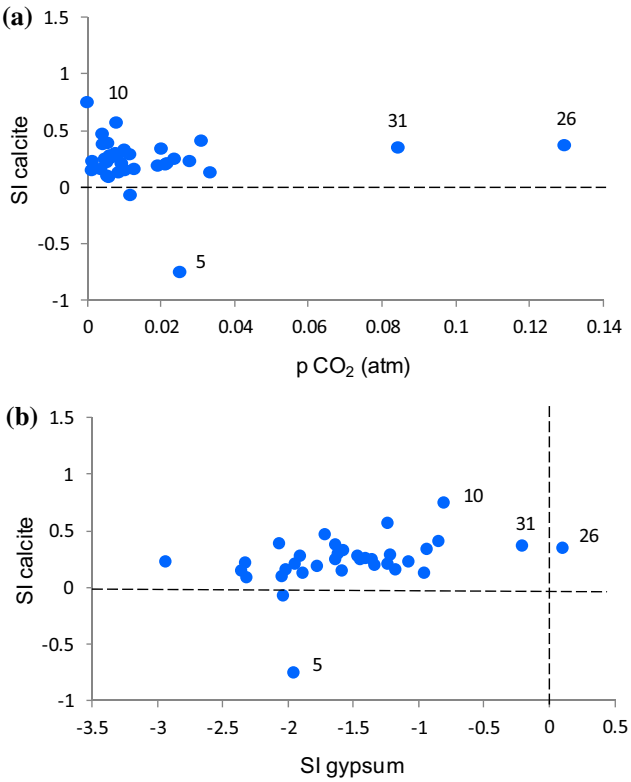

Fig. 5 Plots showing relations between the calcite saturation index (SI) and partial pressure of CO_2 (**a**), and the gypsum SI (**b**) in the studied waters. Dashed lines show equilibrium conditions

contributions from marine derived sediments. The B/Cl, Li/Cl, Sr/Cl and Rb/Cl molar ratios in the studied groundwater samples were generally higher than the corresponding values in seawater (Fig. 8), which is consistent with the Na enrichment shown in Fig. 4a. These findings indicate predominant sources from the dissolution of silicate minerals, rather than marine sediments and/or seawater, and suggest relatively long time of water–rock interaction.

4.5 Geothermometry

As well known, most of chemical geothermometers do not work properly in systems at low temperature (Ármannssòn 2012). The main reason is because thermal occurrences rarely discharge directly from geothermal reservoirs without re-equilibration and/or dilution by meteoric water while crossing shallower aquifers (Minissale 2018). According to the ternary diagram Na–K–Mg proposed by Giggenbach (1988), shown in Fig. 9, most of the Campidano waters resulted in the field of immature water, suggesting disequilibrium with respect to host rock minerals. Groundwater samples No. 3 and No. 30 showed partial equilibrium, whereas the hot sample No. 10 at full equilibrium was an exception (Fig. 9). Taking into account the above findings, chemical geothermometers were only considered for the No. 10 groundwater. According to PHREEQC modeling, this water resulted saturated with respect to chalcedony and quartz. The temperature calculated by the chalcedony and quartz geothermometers (Fournier 1977) was 51 °C and 92 °C, respectively. This result was in line with the temperature shown by the Giggenbach triangular diagram of Fig. 9. It should be remembered that the temperature estimated by the silica geothermometers may indicate only the average temperature of a relatively shallow aquifer, whereas deeper eventual aquifers at higher temperature may occur (Fournier 1977). Temperatures calculated by the Na–K–Ca geothermometer (Fournier and Truesdell 1973) were 60 °C and 88 °C, respectively assuming equilibration below 100 °C (i.e. $\beta = 4/3$) and above 100 °C (i. e. $\beta = 1/3$).

5 Conclusion

In the southern part of the Campidano Graben, hydrogeological, isotopic and geochemical data and chemical modeling allowed to draw the groundwater paths described as follows. Rain infiltration and groundwater circulation at relatively shallow depth (100–200 m b.g.l.) would occur mainly in

Author's personal copy

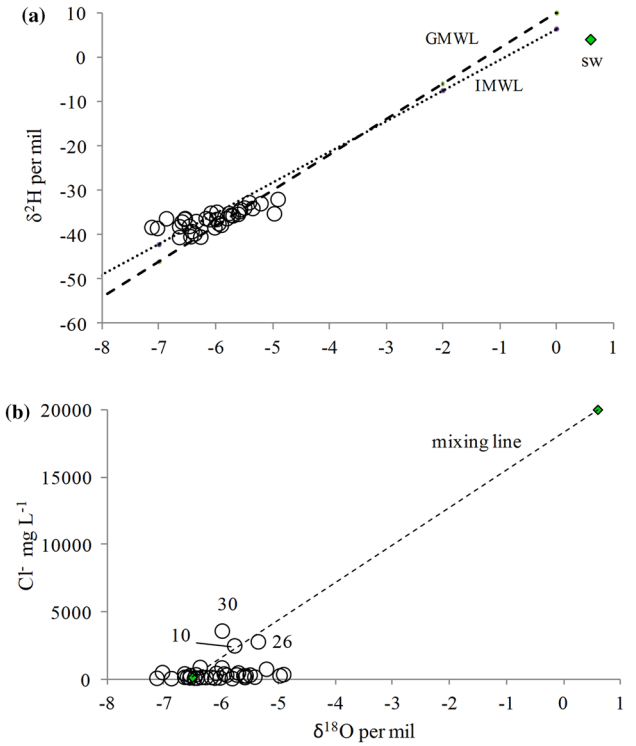

Fig. 6 **a** Plot showing the δ^2H and $\delta^{18}O$ values in the Campidano waters. GMWL is the global meteoric water line (Craig 1961); IMWL is the Italian meteoric water line proposed for the southern Italy (Giustini et al. 2016); sw is the isotopic composition of local seawater (Cidu et al. 2001). **b** Plot showing chloride concentrations and $\delta^{18}O$ values together with the mixing line between freshwater and seawater

the NE sector of the study area, as indicated by well depths (Table 1) and piezometric contour lines in Fig. 2. In this sector, the water interacts with the predominant silicate rocks of the outcropping Paleozoic basement and with Tertiary-Quaternary sediments (sand and sandstone) derived from its alteration, and corresponding to the hydrogeological units PLQ, OM and EO. This interpretation was consistent with EC values ≤ 1 mS cm^{-1}, relatively high DO, relatively low temperature and Cl^-, and very low concentrations of trace elements—such as Li, B, Ge, Cs—that usually increase with increasing temperature and/or the time of water–rock interaction. Underground circulation would deepen as the groundwater flows towards the SW sector, likely reaching the Paleozoic basement underneath the Tertiary–Quaternary formations. This interpretation was supported by relatively high temperature and high values of EC, Cl^- and trace elements observed in groundwater in the SW sector. The above findings are in accordance with results of previous studies carried out at the thermal water Su Campu (Frau 1993, 1994) that indicated a groundwater evolution in a CO_2-closed system, with infiltration and deepening into Paleozoic formations (mainly granitic rocks) or Tertiary sediments formed by granite alteration, and interaction of water with Oligo–Miocene volcanic rocks during the rising path to the surface.

The SW sector of the study area (municipalities of San Sperate and Monastir in Fig. 2) appeared the most promising for the low-enthalpy geothermal exploitation. At Su Campu (42 °C at the groundwater outflow), deep temperatures calculated by silica and Na–K–Ca geothermometers were 51 °C and 60 °C, respectively assuming chalcedony as the controlling phase of silica dissolution and equilibration at temperature below 100 °C. Deep temperatures calculated by quartz dissolution and assuming equilibration at temperature above 100 °C were close to 90 °C. Much higher temperatures appear unlikely to occur in the thermal reservoir. This consideration is consistent with $\delta^{18}O$ values that do not highlight isotopic exchange between oxygen in water and oxygen in minerals, a process occurring at high temperature.

The depth of the thermal reservoir is unknown, however, some information might be inferred by some characteristics of the warmest water no. 10. A very low pCO_2 value and reduced conditions suggest water circulation far from the atmosphere and soil influence. The chemical composition indicates the interaction of water with predominant silicate minerals, which weathering requires long circulation time. Concentrations of major, minor and trace components appear nearly constant over the last 30 years, thus unaffected by recent climatic variations, which in turn also suggest long circulation time. Such observations appear consistent with literature results indicating thermal occurrences in the Campidano Graben as related to the rise up of deep fluids along faults or fractured zones in the granitic–metamorphic complex, i.e. the Paleozoic basement (Angelone et al. 2005). According to geological cross-sections drawn in the South Sardinia (Casula et al. 2001) and the geothermal gradient estimated by linear interpolation of temperatures measured in wells located nearby the study area (Loddo et al. 1982), the thermal reservoir might be located at a depth > 1 km.

To prevent negative impacts on the environment and the human health caused by geothermal exploitation, especially in the case of using the thermal water in spa treatments and balneology, the geothermal effluents should be properly managed. Results on hydrogeochemical characterization indicate that concentrations of toxic and/or harmful components, such as As, B, F^- and Cl^-, may occur in groundwater of the SW sector at concentrations higher than legal limits. Therefore, the geothermal effluents should be either re-injected into the thermal reservoir or adequately treated before discharge.

Author's personal copy

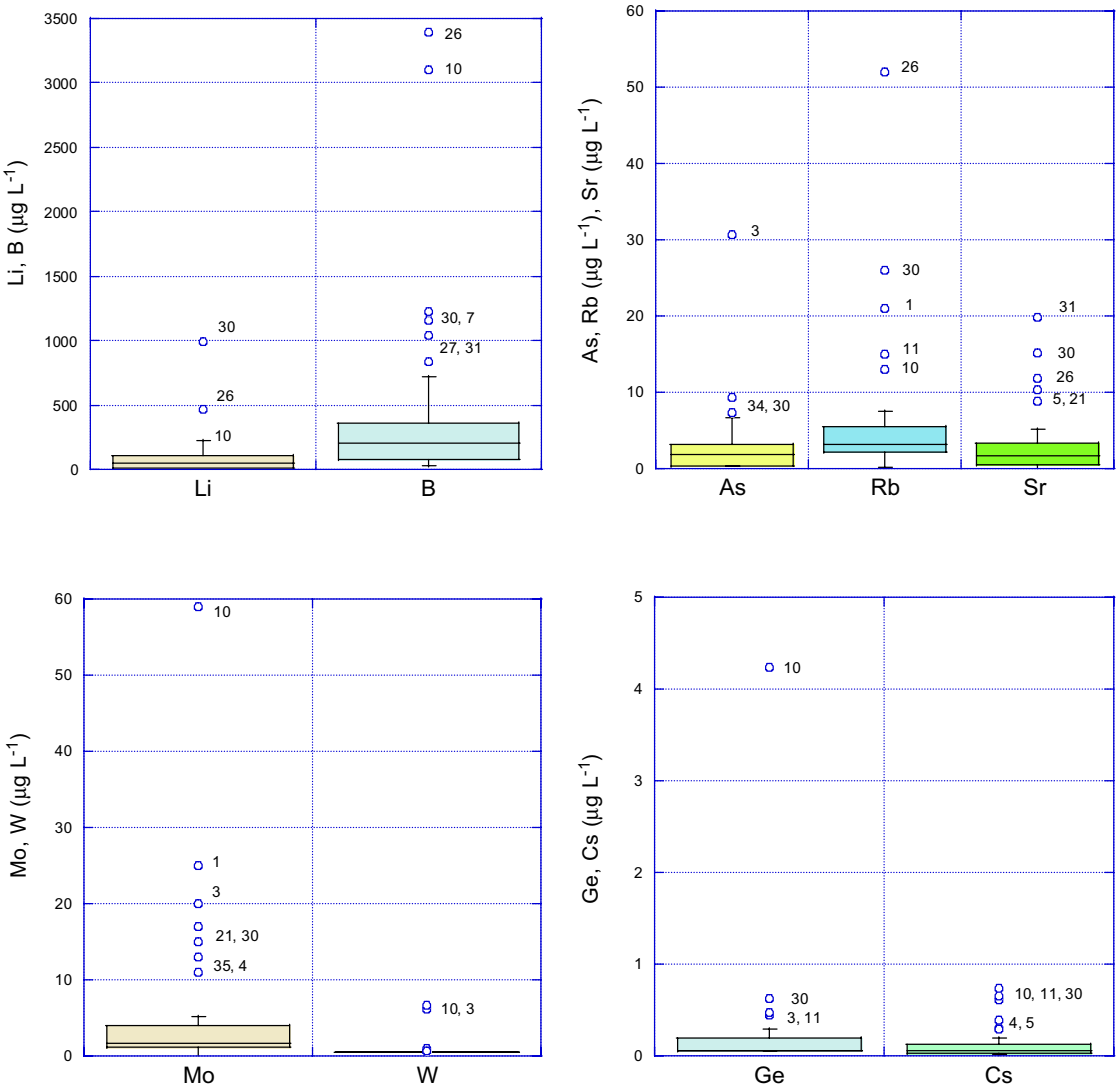

Fig. 7 Box-Plots showing the distribution of selected trace elements in the studied waters

Author's personal copy

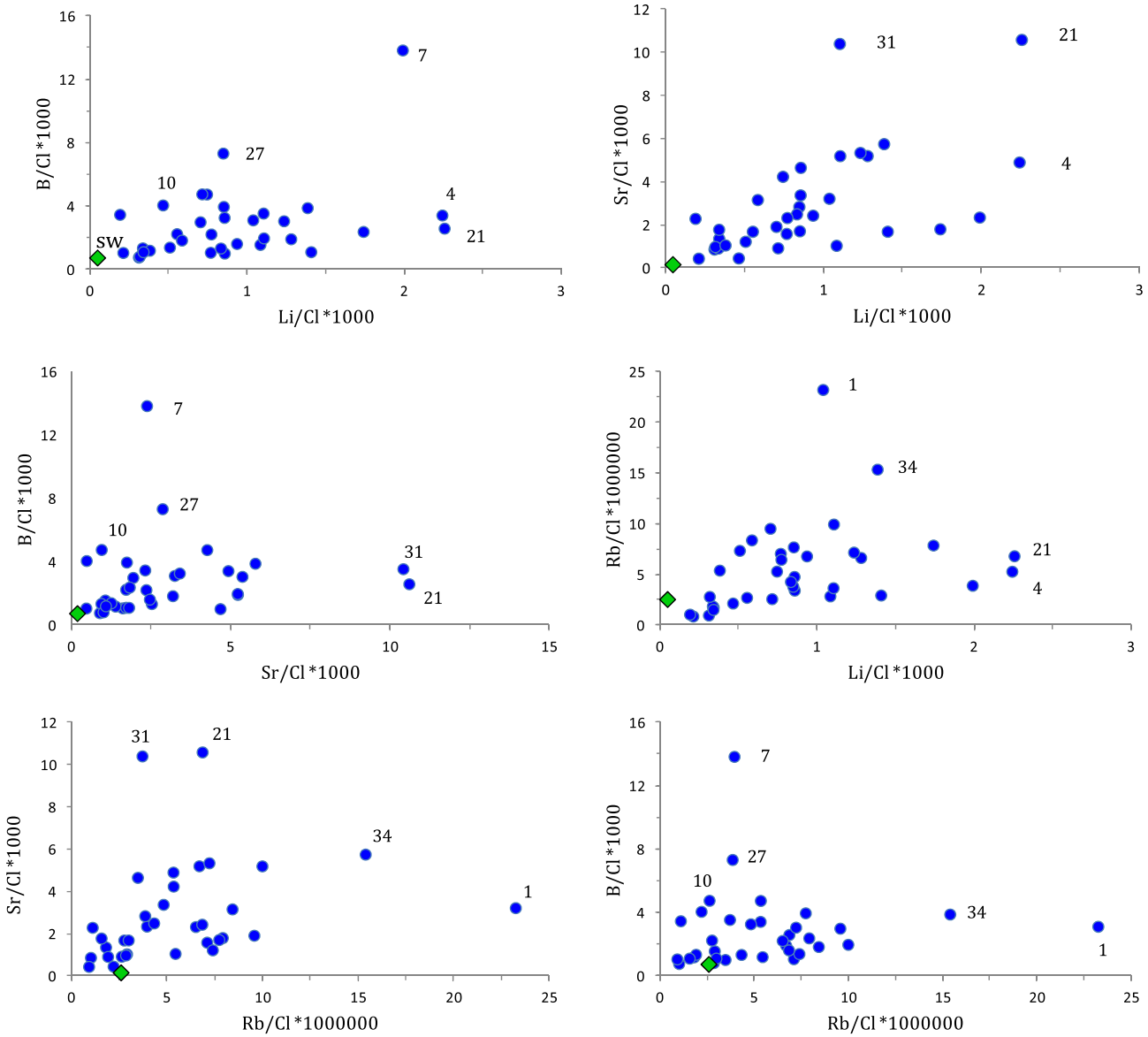

Fig. 8 Plots showing relations between B/Cl^-, Li/Cl^-, Rb/Cl^- and Sr/Cl^- molar ratios in the studied waters as compared to the corresponding values in seawater (sw)

Author's personal copy

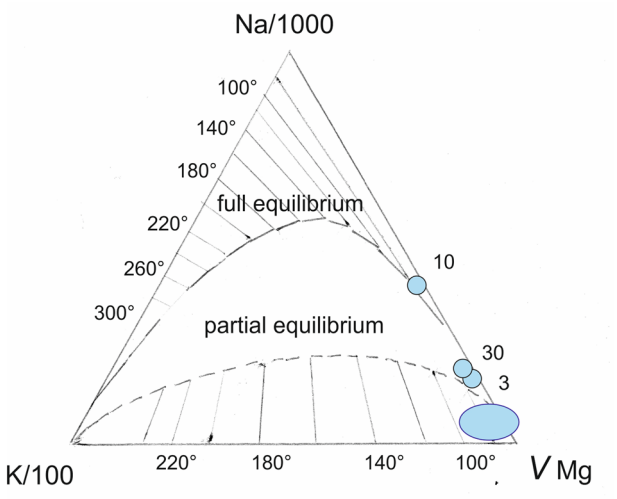

Fig. 9 Ternary diagram Na/1000, K/100, √Mg (Giggenbach 1988, modified) showing equilibrium conditions in the studied waters. The water No. 10 lies on the full equilibrium line, No. 3 and No. 30 show partial equilibrium, whereas all other samples are immature waters. Temperatures are in °C

Acknowledgements Research funded by the Fondazione di Sardegna (Project GETHERE, grant number F71/17000190002, Scientific Responsible P. Valera) and the Autonomous Region of Sardinia (Regional Law 7/2007 CRP 2_114_1, Scientific Responsible L. Fanfani and F. Frau). Thanks to Dr Carlo Calledda who contributed in field and lab work during his master thesis in Geological Sciences at the University of Cagliari, and Dr Claudio Arras for drawing Fig. 1. Thanks to the Editor and Reviewers for their useful suggestions.

References

Angelone M, Gasparini C, Guerra M, Lombardi S, Pizzino L, Quattrocchi F, Sacchi E, Zuppi GM (2005) Fluid geochemistry of the Sardinian Rift-Campidano Graben (Sardinia, Italy): fault segmentation, seismic quiescence of geochemically 'active' faults, and new constraints for selection of CO_2 storage sites. Appl Geochem 20:317–340

Ármannssòn H (2012) Geochemical aspects of geothermal utilization. In: Sayigh A (ed) Comprehensive renewable energy, vol 7. Elsevier, Oxford, pp 95–168

Balia R, Ciminale M, Loddo M, Pecorini G, Ruina G, Trudu R (1984) Gravity survey and interpretation of Bouguer anomalies in the Campidano geothermal area (Sardinia, Italy). Geothermics 13:333–347

Balia R, Cidu R, Pala A, Ranieri G, Serra S (1985) Studio idrogeologico e geochimico delle sorgenti termali di S. Maria is Acquas presso Sardara (Sardegna). In: Atti V Congr. Intern. Acque Sotterranee, Taormina, pp 1–24 (**in Italian**)

Balia R, Ciminale M, Loddo M, Patella D, Pecorini G, Tramacere A (1991) A new geophysical contribution to the study of the Campidano geothermal area (Sardinia, Italy). Geothermics 20:147–163

Bertorino G, Caboi R, Caredda AM, Cidu R, Fanfani L, Panichi C, Sitzia R, Zuddas P (1982a) Idrogeochimica del Graben del Campidano. Report CNR N. CNR-PFE-SPEG-RF-10, CNR Pisa, pp 104–123 (**in Italian**)

Bertorino G, Caboi R, Caredda AM, Cidu R, Fanfani L, Sitzia R, Zuddas P (1982b) Alcune considerazioni sulla geochimica delle acque del Campidano. Report CNR N. CNR-PFE-SPEG-RF-10, CNR Pisa, pp 133–143 (**in Italian**)

Biddau R, Cidu R, Lorrai M, Mulas MG (2017) Assessing background values of chloride, sulfate and fluoride in groundwater: a geochemical-statistical approach at a regional scale. J Geochem Exploration 181:243–255. https://doi.org/10.1016/j.gexplo.2017.08.002

Caboi R, Cidu R, Fanfani L, Pecorini G, Zuddas P (1983) Preliminary geologic and geochemical data for the evaluation of geothermal potential in Sardinia. In: Strub AS, Ungemach P (eds) European geothermal update. Reidel, Kufstein, pp 206–213

Caboi R, Cidu R, Fanfani L, Zuddas P, Zanzari AR (1993) Geochemistry of the high-PCO_2 waters in Logudoro, Sardinia, Italy. Appl Geochem 8:153–160

Carmignani L, Todisco A, Petrone F, Bencini R, Cirese E, Ferri F, Funiciello R, Giardini G, Giusta E, Gisotti G, Graziano R, Pantaleone NA, Rossi M, Scalise AR, Sciotti M, Ventura G, Bianchi M, Vatovec ML (2001) Geologia della Sardegna—Note Illustrative della Carta Geologica della Sardegna a scala 1:200.000—Memorie descrittive della Carta Geologica d'Italia - LX. Ed. Istituto Poligrafico e Zecca dello Stato, Roma (**in Italian**)

CASMEZ (1976) Studio organico delle risorse idriche sotterranee della Sardegna—II fase [Study of groundwater in Sardinia—2nd phase], Università degli Studi di Sassari, Cassa per il Mezzogiorno, Prog. Cassa 25/96 (**in Italian**)

Casula G, Cherchi A, Montadert L, Murru M (2001) The cenozoic graben system of Sardinia (Italy): geodynamic evolution from new seismic and field data. Mar Petrol Geol 18:863–888

Cataldi R, Mongelli F, Squarci P, Taffi L, Zito G, Calore C (1995) Geothermal ranking of Italian territory. Geothermics 24:115–119

Cherchi A, Montadert L (1982) Oligo-Miocene rift of Sardinia and the early history of the Western Mediterranean Basin. Nature 298:736–739

Cidu R (1996) Inductively coupled plasma—mass spectrometry and—optical emission spectrometry determination of trace elements in water. At Spectrosc 17:155–162

Cidu R, Biagini C, Fanfani L, La Ruffa G, Marras I (2001) Mine closure at Monteponi (Italy): effect of the cessation of dewatering on the quality of shallow groundwater. Appl Geochem 16:489–502

Cidu R, Caboi R, Biddau R, Petrini R, Slejko F, Flora O, Aiuppa A, Parello F, Valenza M (2008) Caratterizzazione idrogeochimica ed isotopica e valutazione della qualità delle acque superficiali e sotterranee campionate nel Foglio 549 Muravera. In: Ottonello G (ed) GEOBASI. Pacini Editore, Pisa, pp 149–183 **ISBN 978-88-7781-926-02008 (in Italian)**

Cocco F, Funedda A, Patacca E, Scandone P (2012) Preliminary note on the structural setting of the central-southern Plio-Quaternary Campidano graben (Sardinia). Rend Online Soc Geol It 22:55–57

Cocco F, Funedda A, Patacca E, Scandone P (2013) Plio-Pleistocene extensional tectonics in the Campidano graben (SW Sardinia, Italy): preliminary note. Rend Online Soc Geol It 29:31–34

Coplen TB (2011) Guidelines and recommended terms for expression of stable-isotope-ratio and gas-ratio measurement results. Rapid Commun Mass Spectrom 25:2538–2560

Craig H (1961) Isotopic variations in meteoric waters. Science 133:1702–1703

D'Amore F, Fancelli R, Caboi R (1987) Observations on the application of chemical geothermometers to some hydrothermal systems in Sardinia. Geothermics 16:271–282

Dansgaard W (1964) Stable isotopes in precipitation. Tellus 16:436–468

Egger A, Demartin M, Ansorge J, Banda E, Maistrello M (1988) The gross structure of the crust under Corsica and Sardinia. Tectonophysics 150:363–389

Faccenna C, Speranza F, D'Ajello CF, Mattei G, Oggiano G (2002) Extensional tectonics on Sardinia (Italy): insights into the arc-back-arc transitional regime. Tectonophysics 356:213–232

Author's personal copy

Fournier RO (1977) Chemical geothermometers and mixing models for geothermal systems. Geothermics 5:41–50

Fournier RO, Truesdell AH (1973) An empirical Na-K-Ca geothermometer for natural waters. Geochim Cosmochim Acta 37:1255–1275

Frau F (1993) Selected trace elements in groundwaters from the main hydrothermal areas of Sardinia (Italy) as a tool in reconstructing water-rock interaction. Miner Petrogr Acta 36:281–296

Frau F (1994) A new hydrothermal manifestation in the Campidano graben, Italy: the Su Campu borehole (Monastir). Miner Petrogr Acta 37:155–162

Frau F, Cidu R, Casu M, Soriga A (2019) Assessing arsenic sources in landfill areas: a case study in Sardinia. Ital J Geosci 138:116–123. https://doi.org/10.3301/IJG.2018.30

G.U.R.I.—Gazzetta Ufficiale della Repubblica Italiana (2006) Decreto legislativo 3 aprile 2006, n. 152 Norme in materia ambientale. Gazzetta Ufficiale della Repubblica Italiana n. 88 del 14–4–2006, suppl. ord. n. 96, Roma (**in Italian**)

Giggenbach WF (1988) Geothermal solute equilibria: derivation of Na-K-Mg-Ca geoindicators. Geochim Cosmochim Acta 52:2749–2765

Giustini F, Brilli M, Patera A (2016) Mapping oxygen stable isotopes of precipitation in Italy. J Hydrol Reg Stud 8:162–181

Guerra I (1981) Struttura crostale della Sardegna sulla base dei dati sismici e gravimetrici. In: Proc. 1st meeting GNGTS, CNR, Roma (**in Italian**)

Li Z-W, Feng X-T, Zhang Y-J, Xu T-F (2018) Feasibility study of developing a geothermal heating system in naturally fractured formations: reservoir hydraulic properties determination and heat production forecast. Geothermics 73:1–15

Loddo M, Mongelli F, Pecorini G, Tramacere A (1982) prime misure di flusso di calore in Sardegna. CNR-PFE-SPEG-RF10, Pisa, pp 181–209 (**in Italian**)

Lund JW, Boyd TL (2016) Direct utilization of geothermal energy 2015 worldwide review. Geothermics 60:66–93

Manzella A, Bonciani R, Allansdottir A, Botteghi S, Donato A, Giamberini S, Lenzi A, Paci M, Pellizzone A, Scrocca D (2018) Environmental and social aspects of geothermal energy in Italy. Geothermics 72:232–248

Minissale AA (2018) A simple geochemical prospecting method for geothermal resources in flat areas. Geothermics 72:258–267

Noorollahi Y, Shabbir MS, Siddiqi AF, Ilyashenko EA (2019) Review of two decade geothermal energy development in Iran, benefits, challenges, and future policy. Geothermics 77:257–266

Nordstrom DK (1977) Thermochemical redox equilibria of ZoBell's solution. Geochim Cosmochim Acta 41:1835–1841

Pala A, Pecorini G, Porcu A, Serra S (1982) Geologia e idrogeologia del Campidano. In: Ricerche Geotermiche in Sardegna, CNR-PFE-SPEG-RF10, CNR-Pisa, pp 87–103 (**in Italian**)

Parkhurst DL, Appelo CAJ (1999) PHREEQC version 2. Water-Resources Investigations Report 99-4259. USGS, Denver

Shortall R, Davidsdottir B, Axelsson G (2015) Geothermal energy for sustainable development: a review of sustainability impacts and assessment frameworks. Renew Sustain Energy Rev 44:391–406

Simler R (2012) Manuel pour DIAGRAMMES, Water Software Quality Hydrochemistry. Laboratorie d'Hydrogéologie d'Avignon, France. https://www.lha.univ-avignon.fr/Fichiers/Manuel%2520DIAGRAMMES.pdf

WHO (2011) Guidelines for drinking-water quality, 4th edn. World Health Organization, Geneva **(ISBN: 978 92 4 154815 1)**

Yasukawa K, Kubota H, Soma N, Noda T (2018) Integration of natural and social environment in the implementation of geothermal projects. Geothermics 73:111–123

Yousefi H, Roumi S, Ármannsson H, Noorollahi Y (2019) Cascading uses of geothermal energy for a sustainable energy supply for Meshkinshahr City, Northwest. Iran Geothermics 79:152–163

Publisher's Note Springer Nature remains neutral with regard to jurisdictional claims in published maps and institutional affiliations.